JOURNAL OF MATERIALS SCIENCE 29 (1994) 4104–4112

# Static fatigue behaviour of linear low-density polyethylenes

J. T. YEH*, C. Y. CHEN, H. S. HONG
*Department of Textile Engineering, National Taiwan Institute of Technology, Taipei, Taiwan 106*

Various thermal histories were utilized to generate samples with the same crystalline microstructure (i.e. degree of crystallinity, supermolecular structure, tie molecule density and lamellar thickness) for linear low-density polyethylenes (LLDPEs) with the same molecular weight, molecular weight distribution and branch frequency but different branch length. The static fatigue properties were found to improve with decreasing applied load for samples with the same type of short-chain branches. The failure time of static fatigue ($t_f$) was found to increase dramatically as the branch length increased. An equation was used to predict $t_f$ from the stress, the branch length and other material parameters. In addition, the initial growth rate of the crack opening displacement and the time required to reach the critical opening displacement at the notch roots of the specimens were observed to decrease and increase, respectively, with increasing branch length. This dramatic improvement in static fatigue properties is attributed to the increasing sliding resistance of the polymer chains through the crystal and through entanglements in the amorphous region as the branch length of LLDPEs increases.

## 1. Introduction

Linear low-density polyethylene (LLDPE) polymers are often used in piping, film and other engineering applications, because of their outstanding mechanical properties such as failure time of static fatigue [1–3] and environmental stress crack resistance [4]. For example, the failure time of the static fatigue ($t_f$) of an ethylene–hexene copolymer is approximately 100 to 1000 times more than that of low-density polyethylene (LDPE) and high-density polyethylene (HDPE) [1–3]. This dramatic improvement in $t_f$ has been attributed to the presence of short-chain branches in the molecules of LLDPEs, which results in an increasing resistance to pulling a molecule through a crystalline region compared to that of a smooth molecule [1].

Although they are very few, more detailed investigations [4–6] have indicated that the length and frequency of the short-chain branches have a profound effect on the static fatigue properties of LLDPEs. Focusing on these few publications, the branch frequency has been reported to exhibit a beneficial influence on the static fatigue properties of LLDPE polymers [5]. For instance, the failure time of static fatigue of several ethylene–hexene copolymers was found to increase approximately 10 000 times when the branch frequency increases from 0 to 4.6 butyl branches per 1000C [5]. On the other hand, result [4, 6] concerning the influence of branch length on the static fatigue properties of LLDPEs are varied and contradictory. For example, Bubeck and Becker [4] reported that the environmental stress crack resistance and creep resistance increase when the branch length of LLDPE increases from one to six carbons. However, the branch frequency, molecular weight and molecular weight distribution associated with these samples were not mentioned in this study. Another study reported [6] that the failure time of static fatigue was found to decrease about 100 times when the branch length increases from four to six carbons. However, the weight-average molecular weight ($M_w$) associated with the sample of ethylene–octene copolymer was lower than that of ethylene–hexene copolymer (128 000 versus 170 000), and the molecular weight distribution (MWD) associated with these two copolymers was different, i.e. 1.4 and 11.3 for ethylene–octene and ethylene–hexene, respectively.

In addition to these molecular structure variables (i.e. $M_w$, MWD, branch length and branch frequency), the crystalline microstructure (e.g. tie molecule density $f_T$, degree of crystallinity $W_c$ and spherulite size $D$) was also found to exhibit a profound influence on the dynamic [7–16] and static [3, 5, 17] fatigue behaviour of crystalline polymers. A change in molecular structure variables (i.e. $M_w$, MWD, branch length and branch frequency) or a different thermal history is more or less related to a possible alteration of other microstructural parameters such as tie molecule density, degree of crystallinity and supermolecular structure. For example, $f_T$ is expected to increase with

*To whom all correspondence should be addressed.



0022–2461 

increasing molecular weight [10, 11, 18–21] and branch frequency [5] and, under typical crystallization conditions (e.g. quenching or slow cooling from the melt), the crystallization rate at a given temperature decreases as the molecular weight or branch frequency increases and this generally leads to a decrease in $W_c$ with increasing $M_w$ or branch frequency.

The influence of molecular weight [22, 23], branch frequency [24] and branch length [4] on supermolecular structure is another consideration. However, the molecular structure variables and the full range of microstructural parameters associated with the samples in previous studies have rarely been prepared in a controlled manner, so conclusions concerning the influence of branch length are likely to reflect the influence of other molecular structure variables and microstructural parameters as well. Strictly speaking, the effect of branch length on the static fatigue properties of LLDPE polymers has not been successfully differentiated from that of other molecular structure variables and crystalline microstructure. In this study, various thermal histories were utilized to generate samples with the same crystalline microstructure for a series of LLDPEs with the same weight-average molecular weight, molecular weight distribution and branch frequency but different branch length. The effect of branch length has been isolated and found to have a profound influence on the static fatigue properties of LLDPE polymers.

## 2. Experimental procedure

### 2.1. Materials and preparation

Single-edge notched (SEN) tensile specimens were prepared from ethylene–butene, ethylene–hexene and ethylene–octene copolymer resins with 18 ethyl, butyl and hexyl branches per 1000C, respectively. These resins were kindly supplied by USI Far East Corporation. The molecular weight and its distribution associated with the LLDPEs are shown in Table I. The various thermal histories associated with the series of samples are also summarized in Table I. The samples prepared from ethylene–butene, ethylene–hexene and ethylene–octene copolymers will be referred to as samples A, B and C, respectively. Before sample preparation, these resins were dried in an oven at 80 °C for one hour. The dried resins were then injection-moulded as rectangular plaques with dimensions of 75 mm × 80 mm × 10 mm at temperatures ranging from 90 to 100 °C for various amounts of time. After the required crystallization time the samples were air-cooled to 35 °C.

TABLE I Molecular weights and thermal histories associated with each sample

| Sample | Composition | $M_w$ | $M_w/M_n$ | Thermal history |
|---|---|---|---|---|
| A | Ethylene–butene | $9.2 \times 10^4$ | 3.4 | Isothermal crystallization at 100 °C/12 h |
| B | Ethylene–hexene | $9.4 \times 10^4$ | 3.3 | Isothermal crystallization at 90 °C/1 h |
| C | Ethylene–octene | $9.7 \times 10^4$ | 3.6 | Isothermal crystallization at 100 °C/1 h |

### 2.2. Characterization

#### 2.2.1. Molecular weight and molecular weight distribution

The molecular weight and its distribution associated with LLDPEs were determined by gel permeation chromatography (GPC) (Viscotek model Sigma 1.0). The samples were prepared by dissolving in pure decahydronaphthalene ($C_{10}H_{18}$) at 135 °C to reach a final concentration of 1.0 mg ml$^{-1}$. The amount injected was 0.1 ml and the solvent flow 1 ml min$^{-1}$ at 135 °C. Specified molecular weights of narrow fractions of polystyrene were used to calibrate the instrument. The results for $M_w$ and MWD are summarized in Table I. The difference in these values is not significant. Although $M_w$ increases slightly for samples associated with longer branch length, this increase may in fact reflect the increase in length of short-chain branches rather than that of the main chain of LLDPE.

#### 2.2.2. Thermal analysis

The melting behaviour and the degree of crystallinity ($W_c$) of all samples were studied by using a Dupont differential scanning calorimeter (DSC) model 2000. Baselines used in the experiments were adjusted to have a maximum fluctuation of less than 0.04 mW over the temperature range of interest. With these baselines, the maximum variation of the heat of fusion was normally around $\pm 3$ J g$^{-1}$, which resulted in $\pm 1\%$ error in estimating $W_c$. The instrument was calibrated using pure indium. All scans were carried out under flowing nitrogen at a flow rate of 25 ml min$^{-1}$.

Degrees of crystallinity of all samples were estimated using baselines drawn from 40 to 145 °C and a perfect heat fusion of 293 J g$^{-1}$ [25]. Typical sample weights used in DSC experiments were 10 mg for determination of the degree of crystallinity and 0.5 mg for melting point ($T_m$) measurement. For samples of this size and weight, a maximum variation in $T_m$ of $\pm 0.5$ °C was normally observed. All scans were carried out at a heating rate of 20 °C min$^{-1}$.

Lamellar thicknesses were not measured directly, but were estimated from the observed melting temperature using the Gibbs–Thomson equation [26]. A value of 93 erg cm$^{-2}$ (0.93 J m$^{-2}$ [2, 27] for the end-surface free energy, 1 g cm$^{-3}$ [3, 28] for the perfect crystal density and 141 °C [29] for the equilibrium melting temperature were used for the calculation of lamellar thickness.

#### 2.2.3. Supermolecular structure and size

The supermolecular structure of all samples was viewed through crossed polarizers with an Olympus BHSP-300 optical microscope equipped with a PM-

10AD photomicrographic system. Sections 12 μm thick were cut at room temperature from test pieces of LLDPE plaques using a Reichert–Jung Ultracut E Microtome equipped with a glass knife. By drawing lines across the micrograph of each sample, the average sizes of the supermolecular structures can then be calculated as the ratio of the total length of the lines to the total number of supermolecular structures. Normally, three lines were drawn for each estimation. The spherulite size distribution of these samples was represented by the average spherulite size together with its standard deviation.

### 2.2.4. Tie molecule density

In the past, tie molecules have been characterized by using such techniques as transmission electron microscopy [30–37], neutron scattering [38] and nuclear magnetic resonance [39], and by measurement of the brittle fracture strength [17]. However, due to the small dimensions and complexity of the intercrystalline links, these techniques (excluding the last one) do not appear to be suitable for ready analysis of a relatively large number of bulk samples. In this study, tie molecule density was not measured directly, but was evaluated from brittle tensile strength measurements [17] and/or predicted from the chain dimensions [11]. We are not suggesting that the brittle fracture stress or the chain dimension approach provides a precise measurement of the tie molecule density but rather, qualitative information which will allow a comparison between various samples of a given polymer. The brittle tensile strength of dogbone-shape specimens was determined on a Material Test System apparatus at a temperature of about $-110\,^{\circ}C$ and a crosshead speed of $50\ cm\ min^{-1}$. A minimum of four samples of each specimen type were tested and averaged.

Brown and Ward [17] proposed a model which allows one to estimate the fraction of the interlamellar area covered by tie molecules ($f_T$):

$$f_T = \frac{C\sigma_f - \beta E_{iso}}{\beta(E_T - E_{iso})} \quad (1)$$

where $C$ represents the stress concentration, $\beta$ is a constant of proportionality, $E_{iso}$ the Young's modulus for van der Waals' bonds, and $E_T$ the Young's modulus of the tie chains. For purposes of comparison we use $C = 20$, $\beta = 0.1$, $E_{iso} = 8$ GPa and $E_T = 300$ GPa as proposed by Brown and Ward for polyethylene.

In addition, for purposes of comparison, we use chain dimensions of the polymers to estimate the number of tie molecules formed per chain [11], which is an extension of a model proposed recently by Huang and Brown [18]. The model [11] allows one to evaluate "conventional" tie molecules as well as "entangled" tie molecules formed per chain. The number of "conventional" tie molecules formed per chain, $T_1(M)$, in a monodisperse polymer is given as

$$T_1(M) = \frac{1}{3}\int_{2.45L_p}^{\infty} a' I(r, L_p) r^2 \exp(-b'^2 r^2)\,dr \quad (2)$$

The number of "entangled" tie molecules formed per chain, $T_2(M)$, in a monodisperse polymer is given as

$$T_2(M) = \int_{1.22L_p}^{\infty} N a' r^2 \exp(-b'^2 r^2)\,dr \quad (3)$$

$$N = I(V_M/V_{M_c}) \quad (4)$$

where: $L_p$ is the long period, $a'$ and $b'$ are constants, $I(r, L_p)$ is an integer function which takes into account the increasing probability of forming tie molecules with increasing radius of gyration, $r$ is the end-to-end distance of a random coil in the melt, $M$ is the molecular weight of monodisperse polymer and $M_c$ is the critical molecular weight at which the dependence of viscosity on molecular weight changes from 1 to 3.4 power. For polyethylene, $M_c$ has been reported to be equal to 3800 [40]. $N$ is the number of entanglements per chain after crystallization and is assumed to be proportional to the hydrodynamic volume of the molecular chains, $V_M$ and $V_{M_c}$ are the hydrodynamic volumes of the polymer chain with given molecular weights of $M$ and $M_c$, respectively, and $I(V_M/V_{M_c})$ is the integer part of $(V_M/V_{M_c})$.

The overall number of "tie molecules" formed per chain $T(M)$ for a molecular weight of $M$ is then equal to

$$T(M) = T_1(M) + T_2(M) \quad (5)$$

Bulk polymers are not generally monodisperse, and the actual probability of forming a tie molecule per chain must be calculated from the overall molecular weight distribution of a given polymer; i.e. the average probability of forming a tie molecule per chain can be calculated from the summation of the product of $T(M)$ and number percentage of each monodisperse polymer in the distribution.

## 2.3. Mechanical testing

### 2.3.1. Tensile experiments

Dogbone-shaped specimens were machined and polished from injection-moulded plaques according to the dimensions specified by ASTM D638 Type V. All experiments were conducted in tension at $25 \pm 1\,^{\circ}C$ on a Tensilon UTH-3-500 test system, using a strain rate of $100\ mm\ min^{-1}$. The gauge length was 2.54 cm for all samples. A minimum of four samples of each specimen were tested.

### 2.3.2. Static fatigue experiments

The single-edge notched specimens were sectioned and polished from the injection-moulded plaques. The geometry of the single-edged notched tensile specimen is shown in Fig. 1. The notch was made by pressing a fresh blade into the inside surface of the specimen at a constant speed of $50\ \mu m\ min^{-1}$. The specimens have side grooves which are 1 mm in depth. The width of the specimen is chosen to be 25 mm so that, with the aid of the side grooves, the fracture is almost entirely plane strain. The static fatigue instrument allows one to observe the crack openings in both front and profile

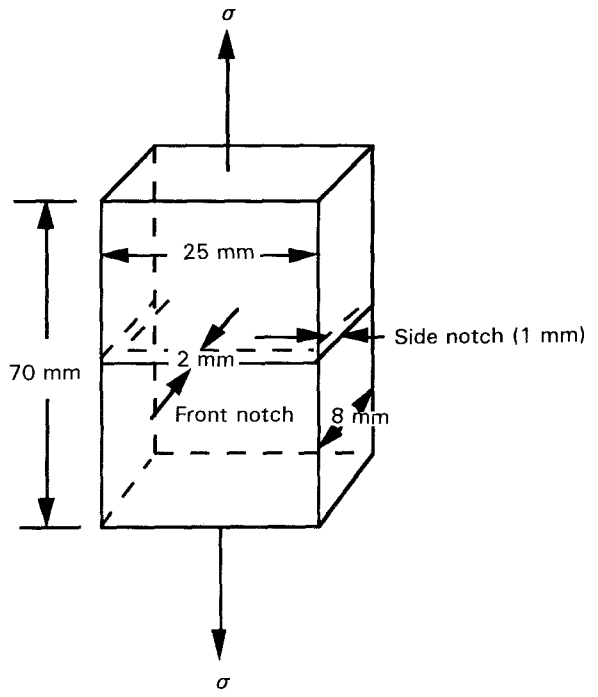


*Figure 1* Shape and dimensions of the single-edge notched tensile specimen.

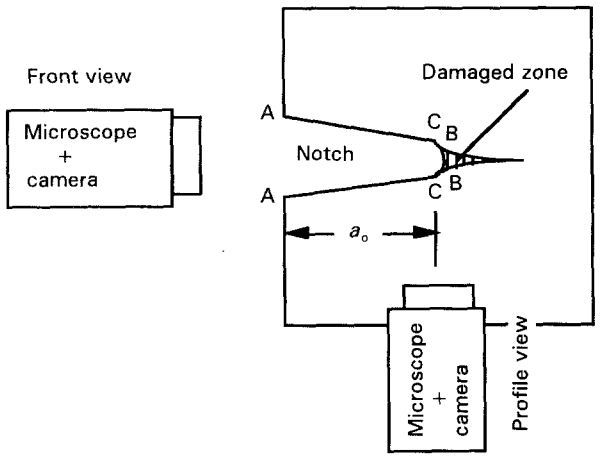


*Figure 2* Experimental measurement of notch opening.

views of the single-edge notched specimens. An Olympus SZ40 optical microscope equipped with an Olympus C35AD-4 photomicrographic system was used to measure the notch openings at the following positions (see Fig. 2): (i) at the surface of the specimen (AA), (ii) at the root of the notch as formed by the razor blade (CC), and (iii) at the base of the craze which is nucleated by the notch (BB). The loading stress ($\sigma$) was calculated as follows:

$$\sigma = F\frac{A_0}{A} \tag{6}$$

where $F$ is the applied force and $A$ and $A_0$ are the notched and unnotched cross-sectional areas. The loading stressed $\sigma$ used in this study was referred to as ligment stress by Lu and Brown in their recent publication [6], and was considered to be a good correlating parameter for predicting the failure time of LLDPE failing in the ductile mode. The specimens were loaded under a constant stress and the temperature was controlled at 25 ± 1 °C.

## 3. Results and discussion

### 3.1. Crystalline microstructure

Microstructural characterization of all samples is summarized in Table II. Approximately the same average spherulite diameter, percentage of crystallinity, calculated lamellar thickness and tie molecule density were found for samples A, B and C. Fig. 3 shows typical optical micrographs of these specimens; the average spherulite diameter was near to 16 μm for each. All these samples exhibited the well-known banded-ring structure. Within experimental error, the percentage of crystallinity ($W_c$) and lamellar thickness ($L$) of all samples are approximately 40% and 14 nm, respectively, which are only about half the values for HDPE as found in our previous work [11]. This is probably due to the presence of the short-chain branches, which prohibits the incorporation of polymer chains into the crystal lattice during crystallization, and results in a lower $W_c$ and $L$.

Tie molecule densities evaluated from measured brittle fracture stresses and predicted from the chain dimensions of samples A, B and C are summarized in Table III. The tie molecule density derived from measurement of brittle fracture stress was ~ 6% and the number of tie molecules formed per chain predicted from the chain dimensions of samples A, B and C was about 26 for all samples. In our previous work [11], the number of tie molecules formed per chain of HDPE samples was predicted to increase from 1.4 to 4.3 when the weight-average molecular weight increased from 30 400 to 132 000. These values are considerably smaller than those predicted for samples A, B and C.

As suggested by Yeh and Runt [11], conventional tie molecules are unlikely to form if the diameter of gyration is less than twice the long period. Similarly, the formation of entangled tie molecules is also unlikely if the diameter of gyration of the polymer chain is smaller than the long period. Based on this premise, the number of the tie molecules formed per chain is expected to decrease with increasing $L$. Since $L$ associated with LLDPE samples is considerably smaller than that of HDPE samples (~ 14 nm versus ~ 23 nm), this dramatic increase in the tie molecule density is not unreasonable. Although both models are indirect and provide only qualitative approach for estimating the number of tie molecules, it still allows one to compare and rank a series of samples. In fact, as

TABLE II Microstructural characterization

| Sample | $W_c$ (%) | $L$(nm) | $D$(μm) |
|---|---|---|---|
| A | 40.1 | 13.0 | 15 ± 3 |
| B | 40.6 | 14.7 | 17 ± 3 |
| C | 41.7 | 13.2 | 16 ± 3 |

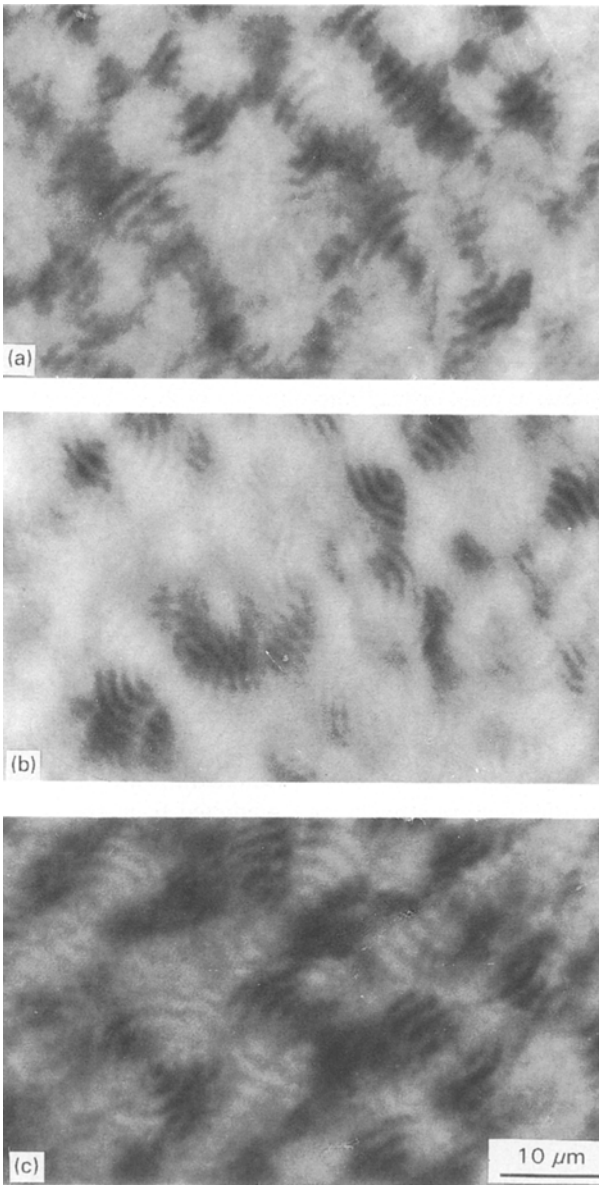


*Figure 3* Optical micrographs of samples (a) A, (b) B and (c) C.

TABLE III Brittle fracture stress and tie molecule density associated with each sample

| Sample | Brittle fracture stress (MPa) | $f_T$ from Equation 1 (%) | $T(M)$ from equation 5 |
|---|---|---|---|
| A | 132 ± 20 | 6.3 | 26.0 |
| B | 130 ± 20 | 6.2 | 26.0 |
| C | 126 ± 20 | 6.0 | 26.3 |

described above, both approaches estimate the same value of tie molecule density for each sample.

## 3.2. Tensile experiments

The tensile properties of the specimens are summarized in Table IV. Within experimental error, no significant change in yield stress was observed for all samples. Typical values of the yield stress of all samples are approximately 14 MPa. In contrast, the fracture work, ultimate strength and elongation increase significantly with increasing branch length of the specimens. Typical strengths and elongations to break were 19 MPa/686%, 25 MPa/849% and 29 MPa/863% for specimens A, B and C, respectively. The fracture work increases from 212 to 292 and 349 kJ for samples A, B and C, respectively.

TABLE IV Tensile properties of the LLDPEs

| Sample | Yield stress (MPa) | Ultimate strength (MPa) | Ultimate elongation (%) | Toughness ($kJ\,m^{-2}$) |
|---|---|---|---|---|
| A | 14 | 19 | 685 | 212 |
| B | 15 | 25 | 849 | 292 |
| C | 14 | 29 | 863 | 349 |

## 3.3. Static fatigue experiments

Fig. 4a shows a typical plot of the kinetics of damage for sample A loaded at 8.5 MPa, where the notch opening at the surface of the specimen ($\delta_{AA}$), at the bottom of the notch ($\delta_{CC}$) and at the thickness of the base of the damage zone ($\delta_{BB}$) are plotted against time. An initial value of the notch opening occurs shortly upon loading the specimen. It is important to note that the initial rate of notch opening ($\delta_0$) is small and nearly constant up to a critical value of $\delta$ (called $\delta_c$), at which fibril fracture occurs. After $\delta_c$, the remaining ligament yields prior to ultimate failure. Similar features of the notch-opening curves were also found by other authors [1–3]. Fig. 4b and c show typical plots of the kinetics of damage for samples B and C loaded at 8.5 MPa, respectively.

In general, the fracture kinetics before fibril fracture occurs is nearly the same for all samples. However, instead of ligament yielding prior to ultimate fracture, the notch openings ($\delta_{AA}$, $\delta_{CC}$, $\delta_{BB}$) of samples B and C increase stepwise before ultimate failure and, during each step, the notch opens very slowly (see Figs 4b and c). In fact, this type of stepwise fracture occurs more frequently as the branch length of the LLDPE increases or the loading stress decreases (Fig. 5). The mechanism associated with the stepwise fracture has been investigated by several authors [41–43]. In a recent study, Lu *et al.* [41] noted the existence of the discontinuities or arrest lines on the fracture surface of an ethylene–octene copolymer which exhibited the stepwise fracture behaviour. The mechanism of stepwise fracture is referred to as "discontinuous crack growth". Some researchers [42] have considered that it was due to a slip–stick mechanism associated with crack blunting, while other workers [41, 43] have attributed the stepwise fracture to the nucleation and growth of voids at the root of a crack in a crystalline solid.

As described previously, the initial slope of the $\delta$–$t$ curve, $\delta_0$, is practically constant up to a critical value $\delta_c$, at which fibril fracture occurs and a marked acceleration of $\delta$ is observed. As shown in Fig. 6, $\delta_0$ obtained from the CC curves decreases significantly

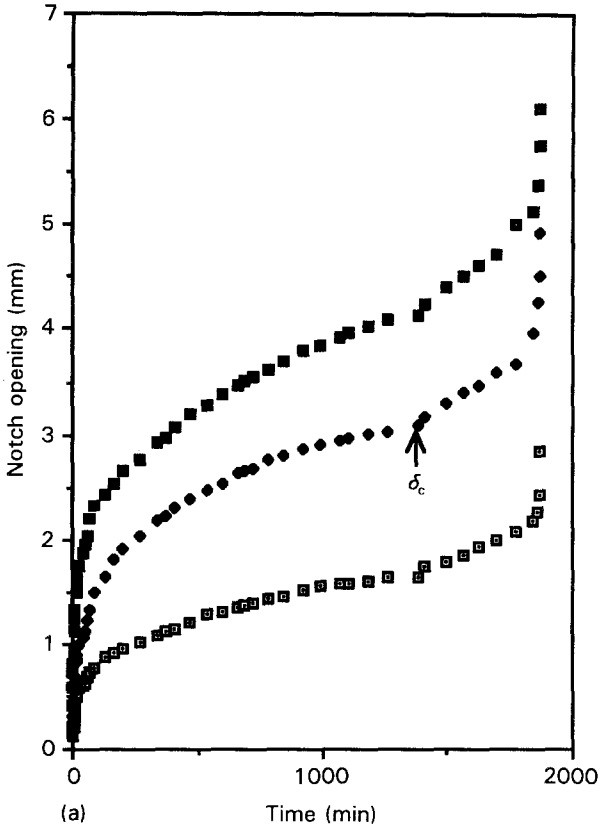


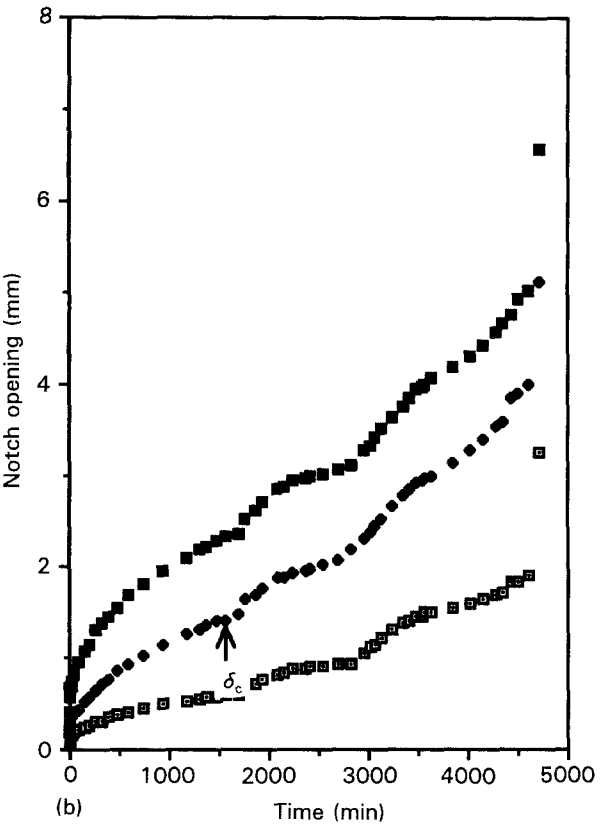


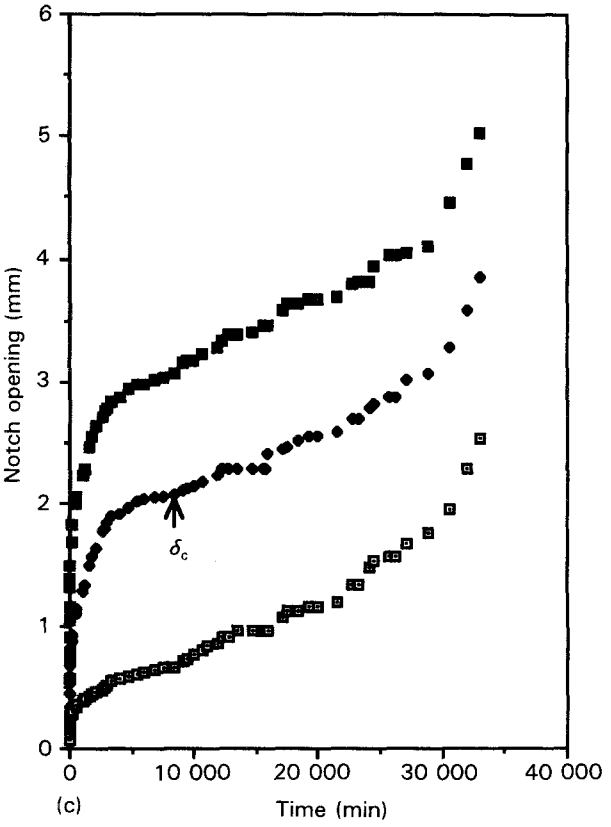


*Figure 4* Notch openings (■) AA, (◆) CC and (⊡) BB plotted against time, tested at 25 °C and 8.5 MPa for (a) ethylene–butene, (b) ethylene–hexene and (c) ethylene–octene copolymer. Arrows indicate when fracture initiated.

with increasing branch length at each loading stress. On the other hand, the time required to reach $\delta_c$ determined at each loading stress increases significantly with increasing branch length and decreases significantly with increasing loading stress (Fig. 7).

Figs 8 and 9 show the plots of failure time $t_f$ versus the loading stress and branch length of each sample, respectively. As expected, the $t_f$ of each copolymer decreases exponentially with increasing the loading stress (see Fig. 8). However, $t_f$ increases significantly with increasing branch length at each loading stress (Fig. 9). For example, at a loading stress of 8.5 MPa, $t_f$ increases from 1878 to 4717 and 39 123 min as the length of short-chain branches increases from two to four and six carbon lengths, respectively. A similar trend was also observed for sample loaded at other stresses. As mentioned previously, the weight-average molecular weight, molecular weight distribution, branch frequency and microstructural parameters (i.e. degree of crystallinity lamellar thickness, supermolecular structure and tie molecule density) within the series remained unchanged. Thus, it is reasonable to suggest that the significant increase in $t_f$ from sample A to B and C is clearly due to the increasing branch length, which in fact increases the sliding resistance of the polymer chains through the crystal and through the entanglements in the amorphous region, and hence results in a decreasing $\delta_0$. This is first time that the influence of the branch length has been isolated from molecular weight, molecular weight distribution, branch frequency and microstructural parameters, and found to exhibit a profound influence on the static fatigue properties of LLDPEs.

In general, for all polyethylenes the most widely used criterion for determining whether the failure is ductile, brittle, or transition is based on the stress ($\sigma$)

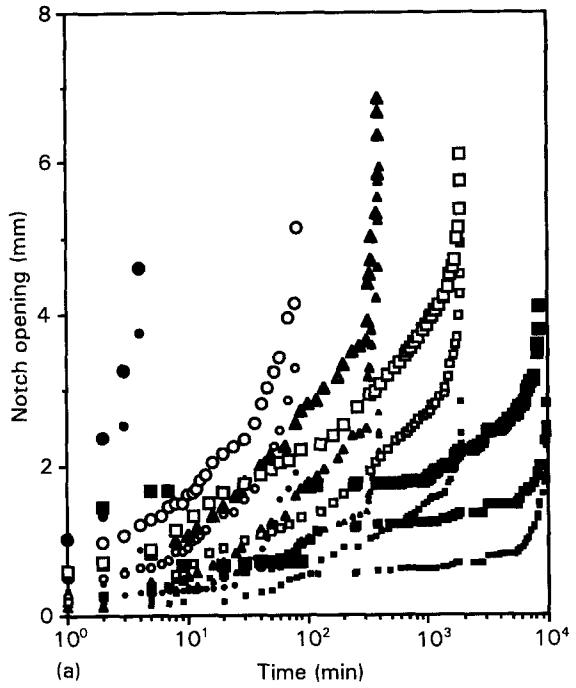


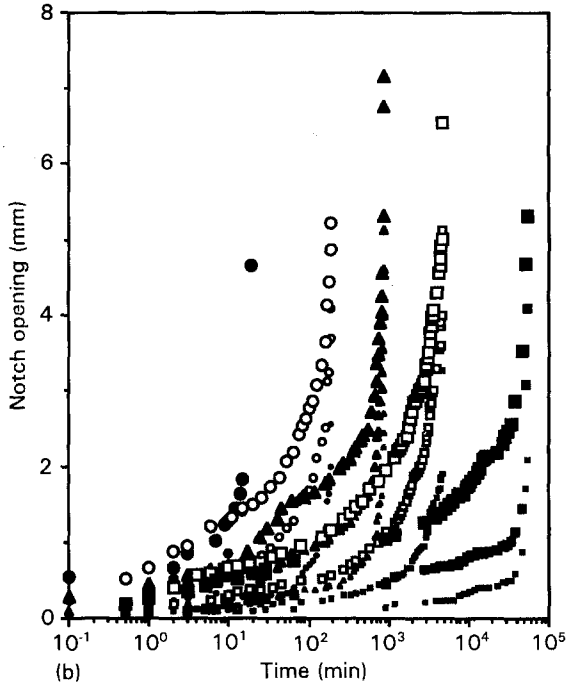


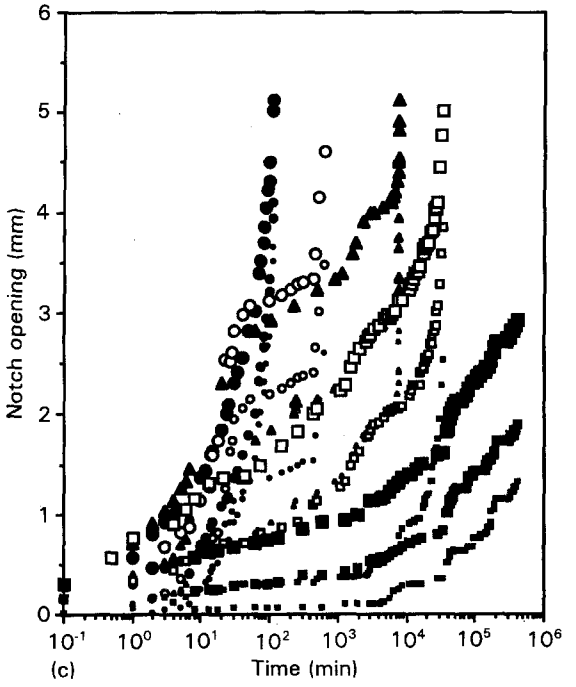


*Figure 5* Notch opening against time for (a) ethylene–butene, (b) ethylene–hexene and (c) ethylene–octene copolymer at various stresses: (●) AA/10 MPa, (●) CC/10 MPa, (●) BB/10 MPa, (○) AA/9.5 MPa, (○) CC/9.5 MPa, (○) BB/9.5 MPa, (▲) AA/9 MPa, (▲) CC/9 MPa, (▲) BB/9 MPa, (□) AA/8.5 MPa, (□) CC/8.5 MPa, (□) BB/8.5 MPa, (■) AA/8 MPa, (■) CC/8 MPa, (■) BB/8 MPa.

against time to failure varying as [44]

$$t_f \propto \sigma^{-n} \tag{7}$$

If $n$ is appreciably greater than about 20, the behaviour is ductile; if less than about 6 the behaviour is brittle. In this study, the value of $n$ is approximate 29.4, 34.8 and 37.5 for samples A, B and C, respectively. Based on this premise, the ultimate fractures for all samples will show ductile behaviour. As mentioned previously, Lu and Brown [6] demonstrated that the ligament stress (i.e. the loading stress used in this study) is a good correlating parameter for predicting the failure time $t_f$ of LLDPEs fractured in the ductile mode, and samples A, B and C are associated with the same material parameters (i.e. $M_w$, MWD, branch frequency, $W_c$, $D$, $L$, and $f_T$) but different carbon

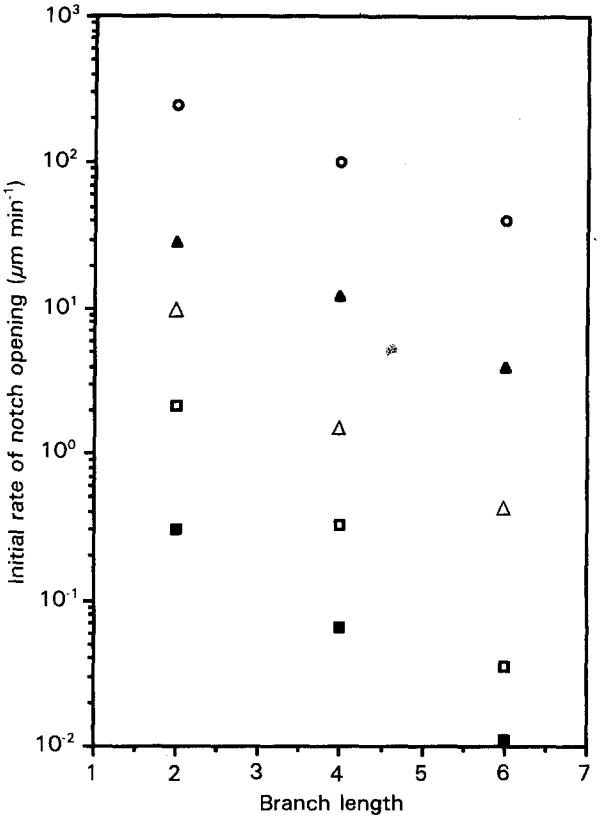


*Figure 6* Initial rate of opening at CC versus the branch length of LLDPE at (■) 8 MPa, (□) 8.5 MPa, (△) 9 MPa, (▲) 9.5 MPa, (○) 10 MPa.

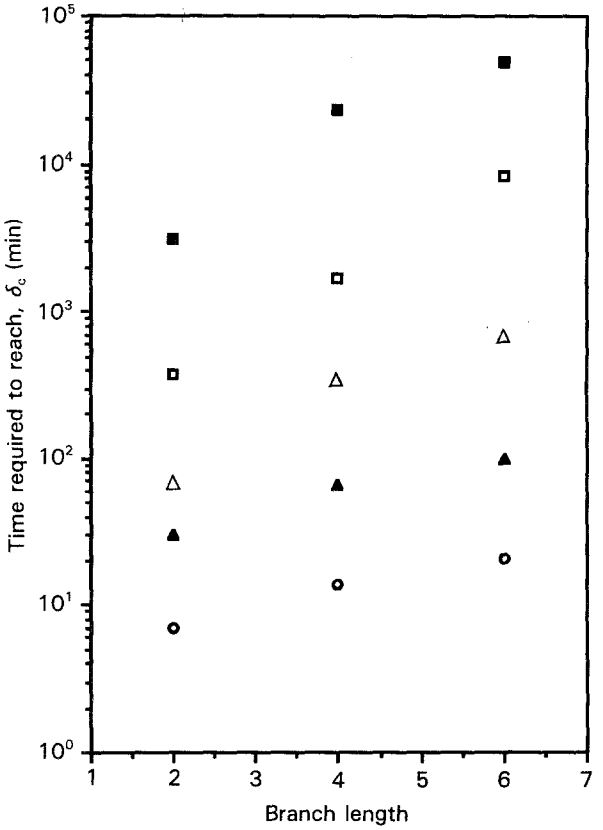


*Figure 7* Time required to reach $\delta_c$ versus the branch length of LLDPE at (■) 8 MPa, (□) 8.5 MPa, (△) 9 MPa, (▲) 9.5 MPa, (○) 10 MPa.

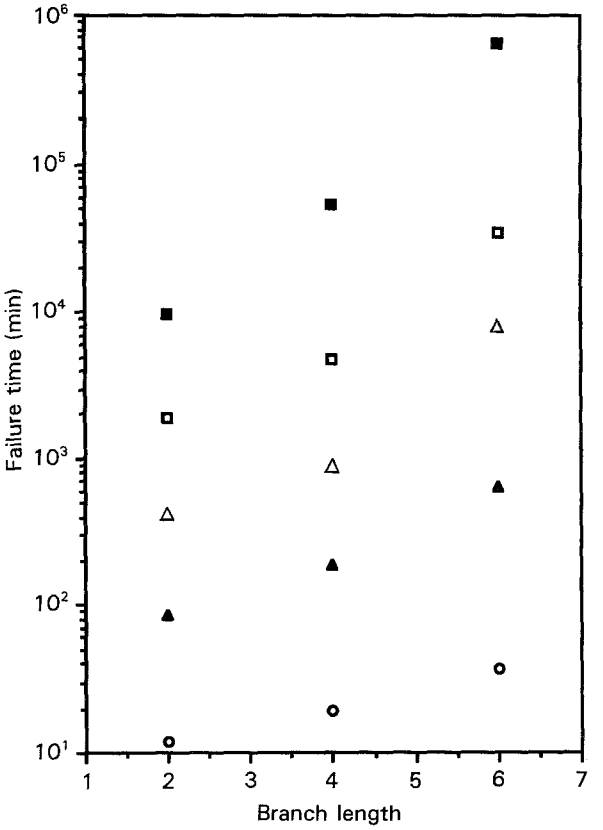


*Figure 9* Failure time versus branch length of LLDPE at (■) 8 MPa, (□) 8.5 MPa, (△) 9 MPa, (▲) 9.5 MPa, (○) 10 MPa.

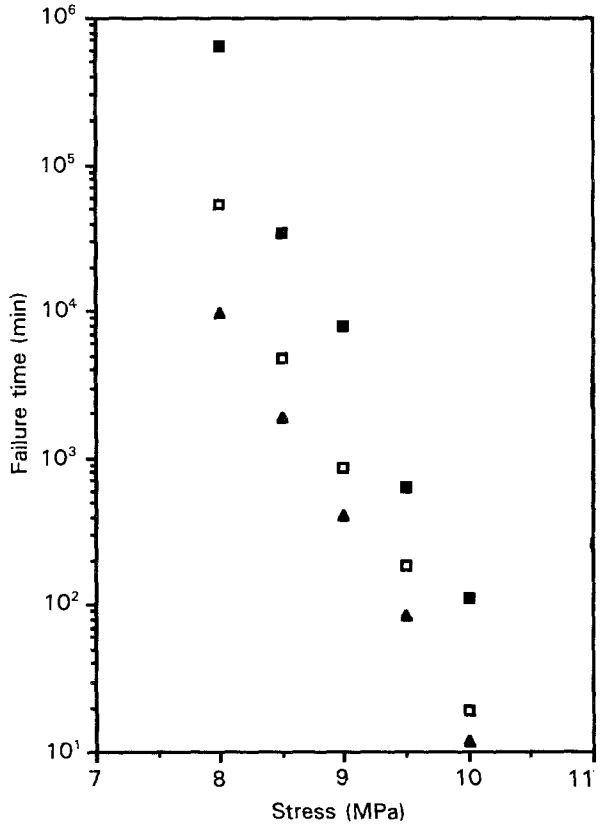


*Figure 8* Failure time versus loading stress for (▲) ethylene–butene, (□) ethylene–hexene, (■) ethylene–octene.

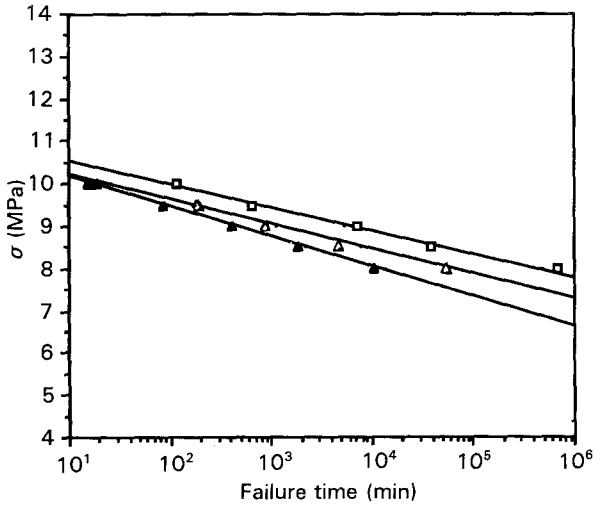


*Figure 10* Loading stress versus failure time for (▲) ethylene–butene, (△) ethylene–hexene, (□) ethylene–octene. The solid lines represent the failure time predicted from Equation 8.

branch lengths. Thus, it is reasonable to suggest that the effect of loading stress and the carbon branch length ($B$) versus $t_f$ is represented by:

$$t_f = AB^m\sigma^{-n} \quad (8)$$

where $A$ and $m$ are constants depending on the material parameters (excluding the branch length) and $n$ equals 29.4, 34.8 and 37.5 for samples A, B and C, respectively. The failure times obtained from experiments and predicted from Equation 8 are shown in Fig. 10, the agreement is within about ± 30% and

should be considered to be very good, since the scatter in the experiment is also about ± 30%.

## 4. Conclusions

Various thermal histories were utilized to generate samples with the same crystalline microstructure (e.g. degree of crystallinity, supermolecular structure, tie molecule density and lamellar thickness) for LLDPEs with the same molecular weight and its distribution and branch frequency, but different branch lengths. As expected, the static fatigue properties were found to improve with decreasing stress for samples with the same branch length. In contrast, the failure time of static fatigue was found to increase dramatically as the branch length of LLDPEs increase. The initial rate of notch opening and the time required to reach $\delta_c$ at the notch roots of the specimens were observed to decrease and increase, respectively, with increasing branch length. This dramatic improvement in static fatigue properties is attributed to the increasing sliding resistance of the polymer chains through the crystal and through the entanglements in the amorphous region as the branch length of LLDPEs increases. The ultimate failure of all samples shows ductile behaviour, since the values of $n$ are greater than 20. Finally, a theoretical equation was developed to describe the failure time in terms of the loading stress, the branch length and other material parameters of LLDPEs. The tolerance of the failure time obtained from experiments and predicted from Equation 8 is within about ± 30%


## Acknowledgements

The authors express their appreciation to the National Science Council (Grant NSC 81-0405-E011-536) for support of this work. Thanks are also extended to Mr Wen-shinann Lee for his assistance in preparation of this manuscript. Last but not least, the authors also express their appreciation to Mr Bruce M.C. Lu of Yung Chia Chemical Industries Corp. for many helpful discussions of this work.


## References


1. X. C. LU, X. Q. WANG and N. BROWN, *J. Mater. Sci.* **23** (1988) 643.
2. X. C. LU and N. BROWN, *ibid.* **21** (1986) 2423.
3. Y. L. HUANG and N. BROWN, *J. Polym. Sci., Polym. Phys. Ed.* **28** (1990) 2007.
4. R. A. BUBECK and H. M. BAKER, *Polymer* **23** (1982) 1690.
5. Y. L. HUANG and N. BROWN, *J. Polym. Sci., Polym. Phys. Ed.* **29** (1991) 129.
6. X. C. LU and N. BROWN, *J. Mater. Sci.* **26** (1991) 612.
7. J. RUNT and K. P. GALLAGHER, *J. Mater. Sci.* **26** (1991) 792.
8. J. A. SANER and G. C. RICHARDSON, *Int. J. Fract.* **16** (1980) 499.
9. J. L. WAY and J. R. ATKINSON, *J. Mater. Sci.* **6** (1971) 102.
10. J. T. YEH and J. RUNT, *J. Mater. Sci.* **24** (1989) 2637.
11. *Idem, J. Polym. Sci., Polym. Phys. Ed.* **29** (1991) 371.
12. J. RUNT and M. JACQ, *J. Mater. Sci.* **24** (1989) 1421.
13. F. X. de CHARENTENAY, F. LAGHOUATI and J. DEWAS, in "Deformation, Yield and Fracture of Polymers" (Plastics and Rubber Institute, London, UK, 1979) p. 61.
14. A. RAMIREZ, J. A. MANSON and R. W. HERTZBERG, *Polym. Eng. Sci.* **22** (1982) 975.
15. K. FRIEDRICH, in *Proceedings of 9th Conference on Scanning Electron Microscopy*, (German Society for Testing Materials (DVM), Stuttgart, 1979) p. 173.
16. A. RAMIREZ, D. M. GAULTIER, J. A. MANSON and R. W. HERTZBERG, in "Fatigue in Polymers" (Plastics and Rubber Institute, London, UK, 1983) p. 31.
17. N. BROWN and I. M. WARD, *J. Mater. Sci.* **18** (1983) 1405.
18. Y. L. HUANG and N. BROWN, *ibid.* **23** (1988) 3648.
19. H. D. KEITH, F. J. PADDEN Jr and R. G. VADIMSKY, *J. Appl. Phys.* **37** (1966) 4027.
20. Y. L. KEITH, F. J. PADDEN Jr and R. G. VADIMSKY, *ibid.* **42** (1971) 4585.
21. S. WELLINGHOFF and E. BAER, *J. Macromol. Sci. Phys.* **B11** (1975) 367.
22. S. M. OHLBERG, J. ROTH and R. A. V. KAFF, *J. Appl. Polym. Sci.* **1** (1959) 114.
23. L. MANDELKERN, M. GLOTIN and R. A. BENSON, *Macromolecules* **14** (1981) 22.
24. D. L. WILFONG and G. W. KNIGHT, *J. Polym. Sci. Polym. Phys. Ed.* **28** (1990) 861.
25. B. WUNDERLICH, in "Macromolecular Physics," Vol. 1 (Academic, New York, 1973) p. 338.
26. J. D. HOFFMAN, G. T. DAVIS and J. I. LAURITZEN, "Treatise on Solid State Chemistry", edited by N. B. Hanmyay, Vol. 3 (Plenum, New York, 1975).
27. J. I. LAURITZEN Jr and J. D. HOFFMAN, *J. Appl. Phys.* **44** (1973) 4340.
28. A. TURNER-JONES, *J. Polym. Sci.* **62** (1962) 53.
29. B. WUNDERLICH, "Macromol. Physics", Vol. 2 (Academic, New York, 1973) p. 388.
30. H. D. KEITH, F. J. PADDEN Jr and R. G. VADIMSKY, *J. Polym. Sci.* Part *A-2* **4** (1966) 267.
31. *Idem, J. Appl. Phys.* **37** (1966) 4027.
32. *Idem, ibid.* **42** (1971) 4027
33. R. G. VADIMSKY, H. D. KEITH and F. J. PADDEN, *J. Polym. Sci.* Part *A-2* **7** (1969) 1367.
34. H. A. DAVIS, *ibid.* **4** (1966) 1009.
35. S. HAGOU and K. AZUMA, *J. Macromol. Sci., Phys. Ed.* **16** (1979) 435.
36. E. S. CLARK, *S. P. E. J.* **23** (1967) 46.
37. H. D. KEITH, F. J. PADDEN Jr and R. G. VADIMSKY, *J. Polym. Sci., Polym. Phys. Ed.* **18** (1980) 2307.
38. E. W. FISCHER, K. HAHN, J. KUGLER, U. STRUTH and R. BOM, *ibid.* **22** (1984) 1491.
39. V. V. ZHIZHENKOV and E. A. EGOROV, *ibid.* **22** (1984) 117.
40. W. W. GRAESSLEY, *Adv. Polym. Sci.* **16** (1974) 55.
41. X. LU, R. QIAN and N. BROWN, *J. Mater. Sci.* **26** (1991) 917.
42. M. K. V. CHAN and J. G. WILLIAMS, *Polymer* **24** (1983) 234.
43. A. W. HESTON, MS thesis, University of Pennsylvania (1983).
44. X. C. LU and N. BROWN, *J. Mater. Sci.* **25** (1990) 411.



*Received 7 August 1992*
*and accepted 29 June 1993*